Symmetry-Protected Topological Metals

Xuzhe Ying[1] and Alex Kamenev[1,2]

[1]*School of Physics and Astronomy, University of Minnesota, Minneapolis, Minnesota 55455, USA*
[2]*William I. Fine Theoretical Physics Institute, University of Minnesota, Minneapolis, Minnesota 55455, USA*

We show that sharply defined topological quantum phase transitions are not limited to states of matter with gapped electronic spectra. Such transitions may also occur between two gapless metallic states both with extended Fermi surfaces. The transition is characterized by a discontinuous, but not quantized, jump in an off-diagonal transport coefficient. Its sharpness is protected by a symmetry, such as, e.g., particle-hole symmetry, which remains unbroken across the transition. We present a simple model of this phenomenon, based on 2D $p + ip$ superconductor with an applied supercurrent, and discuss its geometrical interpretation.

The advent of topological insulators and semimetals [1–5] brought the realization that states of matter may be distinguished by subtle topological indices. The very existence of such indices primarily relies on symmetries of the system, rather than its specific Hamiltonian [5–10]. States with different topological indices are separated by sharp quantum phase transitions (QPT), which are often associated with quantized jumps of certain transport coefficients (such as, e.g., Hall conductance in integer quantum Hall effect [11]). Traditionally, topological QPT are discussed between two gapped phases, e.g., insulators or superconductors. Recently it was realized that Weyl semimetals [12,13] may exhibit genuine QPT between gapless states, if the chemical potential is tuned to a nodal Weyl (or Dirac) point [14,15]. For example, in Weyl semimetals with mirror symmetry, the Hall conductance exhibits a discontinuous quantized jump [16,17].

The goal of this Letter is to point out that the topological transitions are not limited to the gapped states of matter, or to states with the point Fermi surface. Instead, they may persist well into a true metallic state with an extended Fermi surface and a finite density of delocalized states at the chemical potential. Consequently, there are sharp QPTs between topologically distinct metallic (as opposed to semimetallic or insulating) phases. One may dub them *topological metals* (TM) to distinguish them from ordinary metals. Across QPT between TM and a metal, a physical observable, associated with the topological index (e.g., an off-diagonal conductivity), exhibits a discontinuous jump. In contrast to topological QPT in insulators or semimetals, such a jump is *not* quantized. The topological QPT in metals should be necessarily protected by some symmetry. In the absence of any symmetry, the metallic QPT gives way to a smooth crossover, invalidating the sharp designation of the TM phase. Doped Weyl semimetals [13,18–20] (sometimes called topological metals) are usually examples of this latter scenario, as discussed below.

To illustrate these ideas we shall use a two-dimensional (2D) example, which belongs to the symmetry class D [3–5,9,21]. This class is realized, for example, by $p + ip$ superconductors [22–24], which break time reversal symmetry and the only protected symmetry is the particle-hole one. The latter is encoded within the Nambu structure of the corresponding Bogoliubov–de Gennes (BdG) Hamiltonian, $H_{BdG}(\boldsymbol{k})$, where $\boldsymbol{k}$ is a quasi momentum in a 2D Brillouin zone (BZ), as [3,5]

$$P^{-1}H_{BdG}(\boldsymbol{k})P = -H_{BdG}(-\boldsymbol{k}). \qquad (1)$$

Here $P = \sigma_x K$, where K is complex conjugation operator and σ_x is the Pauli matrix in Nambu space with the basis $\Psi_{\boldsymbol{k}} = (c_{\boldsymbol{k}}, c_{-\boldsymbol{k}}^\dagger)^T$. A generic Hamiltonian has a form

$$H_{BdG}(\boldsymbol{k}) = d_0(\boldsymbol{k}) + \boldsymbol{d}(\boldsymbol{k}) \cdot \boldsymbol{\sigma}, \qquad (2)$$

where $d_0(\boldsymbol{k})$ and $\boldsymbol{d}(\boldsymbol{k}) = (d_x, d_y, d_z)$ are functions of momentum. The particle-hole symmetry, Eq. (1), restricts $d_{0,x,y}(\boldsymbol{k})$ to be odd, while $d_z(\boldsymbol{k})$ is even, under $\boldsymbol{k} \leftrightarrow -\boldsymbol{k}$. The spectrum consists of two bands with energies

$$\epsilon_{\boldsymbol{k}}^{(\pm)} = d_0(\boldsymbol{k}) \pm \sqrt{d_x^2(\boldsymbol{k}) + d_y^2(\boldsymbol{k}) + d_z^2(\boldsymbol{k})}, \qquad (3)$$

which may only touch when $\boldsymbol{d} = 0$. In the simplest example of the square lattice [1,25], $d_0 = 0$, $d_x = -2\Delta \sin k_y$, $d_y = -2\Delta \sin k_x$, and $d_z = -2t \cos k_x - 2t \cos k_y - \mu$, where t, μ, and Δ are the hopping parameter, chemical potential, and p wave pairing amplitude, correspondingly. The spectrum (3) is fully gapped everywhere away from the topological QPT. The later takes place at $\mu = \mp 4t$ and results in a gapless point at $\boldsymbol{k} = (0,0)$, or (π, π), correspondingly.

The topological properties stem from the homotopy group $\boldsymbol{Z}$ [3–5] associated with the mapping of the 2D

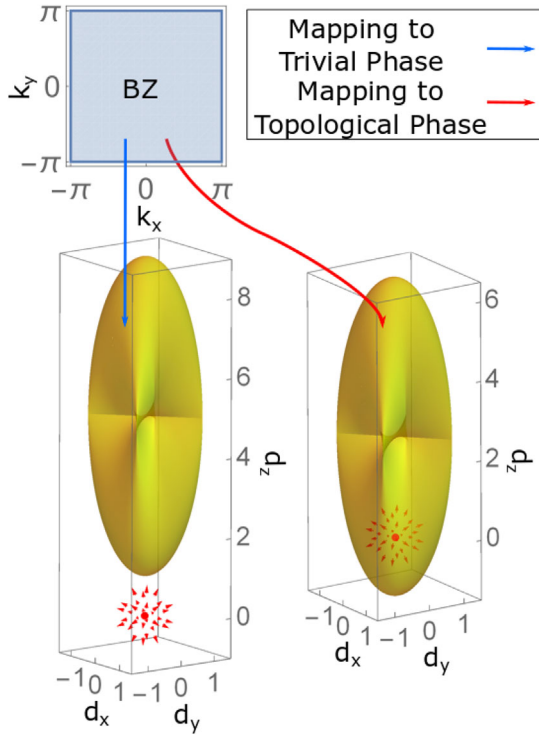FIG. 1. Brillouin zone mapping onto closed $\boldsymbol{d}(\boldsymbol{k})$ surface in 3D $\boldsymbol{d}$ space for $t = 1$, $\Delta = 0.5$. The monopole, located at the origin $\boldsymbol{d} = 0$, is shown in red. Trivial phase is shown for $\mu = -5$, topological phase for $\mu = -2.5$. The Berry flux through the surface is zero in the trivial phase and quantized in units of the monopole charge in the topological phase.

BZ (torus) onto the 3D space spanned by the vector $\boldsymbol{d}$. [Notice that $d_0(\boldsymbol{k})$ component, being commutative with the Hamiltonian, is not related to the topology; it may be important however in assigning occupation numbers to states with momentum $\boldsymbol{k}$.] The image of BZ, $\boldsymbol{k} \in$ BZ, is a closed 2D surface $\boldsymbol{d}(\boldsymbol{k})$ in the 3D $\boldsymbol{d}$ space, with an integer $\boldsymbol{Z}$ wrapping around the gapless point $\boldsymbol{d} = 0$. The topological QPT, associated with the change of the integer wrapping number, occurs if the gapless point $\boldsymbol{d} = 0$ lies on the BZ image (in our example this only happens at $\mu = \mp 4t$), see Fig. 1. In the cylindrical geometry of Fig. 2, the topological index counts a number of gapless chiral modes localized near the two edges of the cylinder.

The physical quantity, sensitive to the topological index, is the intrinsic (anomalous) Hall conductance. In the case of the superconductor, the object of interest is the *thermal* Hall conductance σ_{xy}^{int}, given by the ratio of the thermal current in the x direction to the temperature gradient applied in the y direction, see Fig. 2. It originates from the anomalous velocity of Bloch electrons due to the Berry curvature term [26,27] in the semiclassical equations of motion. According to the Kubo-Středa formula [25,28], the anomalous thermal Hall conductance (in unit of $(\pi k_B^2/12\hbar)T$) is given by the integrated Berry curvature
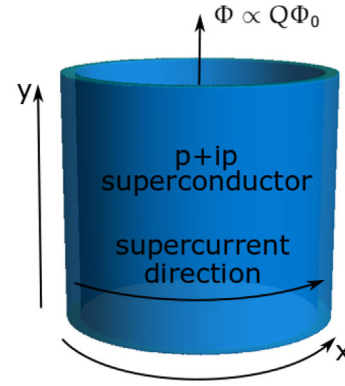

FIG. 2. Schematic geometry of the system discussed in the text.

$$\sigma_{xy}^{\text{int}} = \sum_n \int_{\text{BZ}} \frac{d^2 k}{(2\pi)^2} f(\epsilon_{\boldsymbol{k}}^{(n)}) \Omega_z^{(n)}(\boldsymbol{k}), \qquad (4)$$

where $\Omega_z^{(n)}(\boldsymbol{k})$ is the z component of the Berry curvature, defined as the momentum space curl of the Berry connection $\boldsymbol{\Omega}^{(n)}(\boldsymbol{k}) = \nabla_{\boldsymbol{k}} \times \boldsymbol{\mathcal{A}}^{(n)}(\boldsymbol{k})$ and $\boldsymbol{\mathcal{A}}^{(n)}(\boldsymbol{k}) = \langle u^{(n)}(\boldsymbol{k})|i\nabla_{\boldsymbol{k}}|u^{(n)}(\boldsymbol{k})\rangle$. Here $|u^{(n)}(\boldsymbol{k})\rangle$ is a Bloch wave function in the band n and $f(\epsilon_{\boldsymbol{k}}^{(n)})$ is the Fermi function.

A fully gapped system at a temperature T much less than the gap found in Eq. (4) leads to a quantized anomalous conductance. For example, the gapped two-band model, described by the Hamiltonian (2), results in

$$\sigma_{xy}^{\text{int}} = \int_{\text{BZ}} \frac{d^2 k}{(2\pi)^2} (\partial_{k_x} \boldsymbol{d} \times \partial_{k_y} \boldsymbol{d}) \cdot \frac{\boldsymbol{d}}{2|\boldsymbol{d}|^3}. \qquad (5)$$

This expression may be viewed as a flux of a monopole, located at $\boldsymbol{d} = 0$, through the closed surface $\boldsymbol{d}(\boldsymbol{k})$, see Fig. 1. Indeed, $d^2 k(\partial_{k_x} \boldsymbol{d} \times \partial_{k_y} \boldsymbol{d})$ is the area element of the surface, while $(\boldsymbol{d}/2|\boldsymbol{d}|^3)$ is the field strength of the monopole with the unit "charge." Because of Gauss's law, such a flux is quantized and proportional to the integer wrapping number $\boldsymbol{Z}$ of the BZ image $\boldsymbol{d}(\boldsymbol{k})$ around $\boldsymbol{d} = 0$. This is the essence of the familiar conductance quantization in topological insulators [1,2,29,30].

Let us now modify the model to bring it to the metallic state. The simplest way of doing it is to introduce a magnetic flux Φ through the cylinder of Fig. 2. The flux induces the supercurrent in the x direction, breaking the reflection symmetry, $\epsilon_{-\boldsymbol{k}}^{(n)} \neq \epsilon_{\boldsymbol{k}}^{(n)}$. In the presence of the flux, the order parameter acquires a spatial dependence: $\Delta(x, y) = \Delta e^{iQx}$, where $Q = \Phi/(N\Phi_0)$ with N number of lattice periods around the cylinder [31]. Upon a gauge transformation, this leads to the Hamiltonian (2) with the following parameters:

$$d_0 = 2t \sin k_x \sin Q/2,$$
$$d_x = -2\Delta \sin k_y, \qquad d_y = -2\Delta \sin k_x,$$
$$d_z = -2t \cos k_x \cos Q/2 - 2t \cos k_y - \mu. \qquad (6)$$

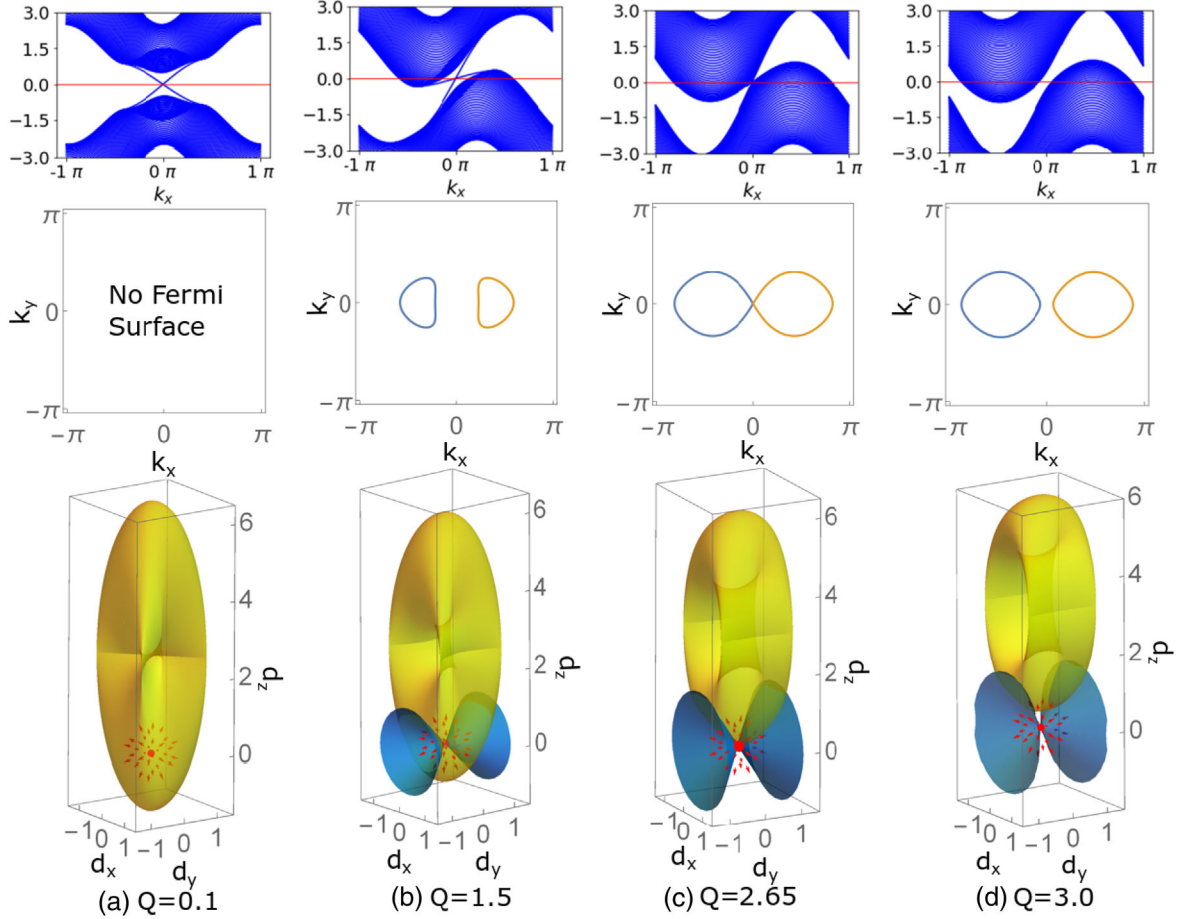FIG. 3. The three rows show spectra as a function of k_x, BZ with the Fermi surfaces, 3D $\boldsymbol{d}$ space with the $\boldsymbol{d}(\boldsymbol{k})$ surface (gold), monopole at $\boldsymbol{d} = 0$ (red) and Fermi double cone, Eq. (7), (blue). The four columns correspond to different values of flux Q: (a) topological superconductor; (b) topological metal; (c) topological QPT; (d) ordinary metal. Figure 5 specifies other parameters.

Notice that the particle-hole symmetry (1) and symmetry class D are still intact and so is the topological quantization of σ_{xy}^{int}, as long as the spectrum (3) remains fully gapped. This is indeed the case for sufficiently small flux $|Q| < Q_L = 2 \arcsin(\Delta/t)$. Figure 3(a) shows spectrum for the cylindrical geometry of Fig. 2, which clearly exhibits chiral edge modes at $Q = 0.1 < Q_L$. It also shows $\boldsymbol{d}(\boldsymbol{k})$ surface, which encloses the monopole at $\boldsymbol{d} = 0$.

At $|Q| = Q_L$ the system undergoes the Lifshitz transition [32,33] into a metallic state. This is shown in the upper row of Fig. 3(b), where one can clearly see two metallic bands: one is particlelike and the other is holelike. The corresponding Fermi surface consists of two disconnected closed curves in the 2D BZ. However, this is *not* yet the topological QPT, as one may notice by the presence of the chiral edge modes in the spectrum of Fig. 3(b). Since the edge modes coexist now with the bulk states at the Fermi level, one does not expect a quantized thermal Hall conductance. Indeed, Eq. (5) for the intrinsic conductance is still valid with the understanding that the integral runs only over the $\boldsymbol{k}$ states with one occupied band (at $T = 0$).

Thus the $\boldsymbol{d}(\boldsymbol{k})$ surface develops two holes—the images of the 2D Fermi curves.

To understand it geometrically, one may notice that $d_0 = -(t/\Delta) \sin(Q/2) d_y$ and therefore the equations for the Fermi curves $\epsilon_{\boldsymbol{k}}^{(\pm)} = 0$ acquire the form [cf. Eqs. (3) and (6)]

$$d_x^2 + \left(1 - \frac{\sin^2(Q/2)}{\sin^2(Q_L/2)}\right) d_y^2 + d_z^2 = 0, \tag{7}$$

where $\sin(Q_L/2) = \Delta/t$. For $|Q| > Q_L$ this condition spells the *double cone* in the $\boldsymbol{d}$ space with the apex at the monopole $\boldsymbol{d} = 0$. The images of the Fermi curves are thus found as the intersections of the cone, Eq. (7), with the closed surface $\boldsymbol{d}(\boldsymbol{k})$, Figs. 3(b)–3(d). The flux of the monopole, which contributes to σ_{xy}^{int}, Eq. (5), is therefore less than the quantized value by the amount of the flux channeled through the cone (7)

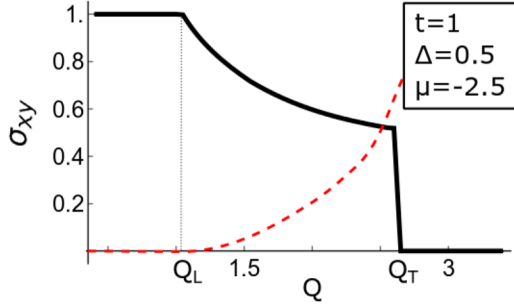$$\sigma_{xy}^{\text{int}}(Q) = \sin \frac{Q_L}{2} \Big/ \left| \sin \frac{Q}{2} \right|, \tag{8}$$

FIG. 4. Thermal Hall conductance (in unit of $(\pi k_B^2/12\hbar)T$) vs flux. Q_L and Q_T are the location of Lifshitz and topological transitions. Solid line—the intrinsic contribution, Eq. (5); dashed line—(schematic) skew-scattering contribution in $T \to 0$ limit.

where $|\sin(Q/2)| \geq \sin(Q_L/2)$, see Fig. 4. The phase diagram of the system is schematically depicted in Fig. 5. At the Lifshitz transition, the system goes from the topological insulator (superconductor) phase to the TM phase. It is characterized by the coexistence of the bulk states at the Fermi level with the chiral edge modes. The latter are responsible for the intrinsic contribution to the thermal Hall conductance, which is *not* quantized.

It turns out that the Lifshitz transition is followed by another transition at $|Q| = Q_T(\mu) > Q_L$, where $\cos(Q_T/2) = 1 - (|\mu|/2t)$. This second transition separates two topologically distinct *metallic* phases. At the transition, the two Fermi curves touch each other at the single point $d = 0$, see Fig. 3(c). On the other side of the transition, the two Fermi curves separate again, see Fig. 3(d), and the edge states disappear. In the 3D d space, the apex of the cone (7) crosses the surface $d(k)$ and the Berry flux of the monopole, Eq. (5), undergoes a discontinuous jump down to zero. The nonquantized height of the jump is given by $\delta\sigma_{xy}^{int} = \sin(Q_L/2)/\sin(Q_T/2) < 1$, cf. Eq. (8).
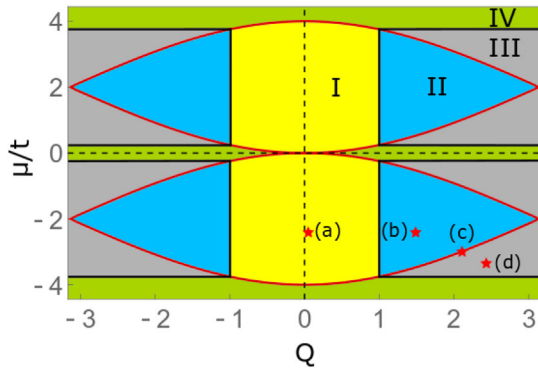

FIG. 5. Phase diagram of the model Eqs. (2) and (6) on chemical potential vs flux plane. I—topological insulator (superconductor); II—topological metal; III—ordinary metal; IV—ordinary insulator. Solid red lines—topological QPT; solid black lines—Lifshitz transitions. Red stars show parameters of columns (a)–(d) in Fig. 3.

The sharp topological QPT at Q_T allows for unambiguous distinction between TM and the ordinary metal states. This sharp distinction is protected by the particle-hole symmetry, Eq. (1). Indeed, since the surface $d(k)$ is punctured by the holes created by the Fermi curves, one may expect the Berry flux and σ_{xy}^{int} to evolve to zero in a smooth, continuous way. This is the case if the gapless point $d = 0$ moves (as a function of some parameter) through one of those Fermi punctures. Such a scenario, invalidating the notion of the sharp TM phase, takes place in doped Weyl semimetals. There the monopole, moving as a function of k_z (the momentum in the direction connecting the two nodes) [13,18,19], goes through the Fermi hole, smearing the topological transition [34].

In our case, the particle-hole symmetry, Eq. (1) (in Weyl materials it is broken by doping), ensures that the $d = 0$ point cannot fall inside any of the Fermi punctures, but can only simultaneously touch both of them. The double cone construction, Eq. (7), is a geometric manifestation of the symmetry (1). It shows that the Berry flux through the punctured $d(k)$ surface must change discontinuously at the topological QPT.

Let us now briefly discuss the role of disorder. The latter has two distinct effects on the discussed phenomena. In the metallic phase (being treated beyond the Born approximation), it generates additional contribution to the thermal Hall conductance, known as the skew scattering [35–41], see Fig. 4. Its specific value depends on the details of the disorder [38,39] and may exceed the intrinsic contribution, discussed here. The important observation is that the skew-scattering contribution, being a bulk phenomenon, is continuous across the topological phase transition at $Q = Q_T$ [42]. It therefore does not alter the discontinuity in σ_{xy}, but merely adds a smooth background.

The second effect of the disorder is associated with the modification of the intrinsic contribution itself. We performed numerical simulations on small (way smaller than the localization length) lattices in the cylindrical geometry [42]. It showed that, for each disorder realization, the discontinuity σ_{xy}^{int} exists, though its location and height fluctuate from one realization to another. In the thermodynamic limit, we expect the Anderson localization to stabilize the topological transition [43–47] in a way similar to the integer quantum Hall effect. However, such a transition separates the now topologically distinct Anderson insulator, rather than metallic, phases. Though a full theory of such a transition in 2D class D [46] is still absent, it is likely that localization restores the quantization of σ_{xy}.

To conclude, we have shown that the sharp definition of the topological states may be extended onto a gapless metallic phase. An unbroken symmetry is required to enforce the identity of such a topological metal state. As an example, we worked out class D [48], $p + ip$ superconductor subject to a supercurrent. The TM phase, protected by the particle-hole symmetry, appears in a

certain finite range of the supercurrent densities. It may be detected by a jump of the thermal Hall conductance, associated with the discontinuous change of the Berry curvature flux.

[1] B. A. Bernevig and T. L. Hughes, *Topological Insulators and Topological Superconductors* (Princeton University Press, Princeton, NJ, 2013).

[2] S.-Q. Shen, *Topological Insulators* (Springer-Verlag, Berlin, 2012).

[3] M. Z. Hasan and C. L. Kane, Rev. Mod. Phys. **82**, 3045 (2010).

[4] X.-L. Qi and S.-C. Zhang, Rev. Mod. Phys. **83**, 1057 (2011).

[5] C.-K. Chiu, J. C. Y. Teo, A. P. Schnyder, and S. Ryu, Rev. Mod. Phys. **88**, 035005 (2016).

[6] S. Ryu, A. P. Schnyder, A. Furusaki, and A. W. W. Ludwig, New J. Phys. **12**, 065010 (2010).

[7] E. P. Wigner, Ann. Math. **67**, 325 (1958).

[8] F. J. Dyson, J. Math. Phys. (N.Y.) **3**, 1199 (1962).

[9] A. P. Schnyder, S. Ryu, A. Furusaki, and A. W. W. Ludwig, Phys. Rev. B **78**, 195125 (2008).

[10] J. Kruthoff, J. de Boer, J. van Wezel, C. L. Kane, and R.-J. Slager, Phys. Rev. X **7**, 041069 (2017).

[11] *The Quantum Hall Effect*, edited by R. E. Prange and S. M. Girvin (Springer-Verlag, New York, 1987).

[12] P. Hosur and X. Qi, C.R. Phys. **14**, 857 (2013).

[13] N. P. Armitage, E. J. Mele, and A. Vishwanath, Rev. Mod. Phys. **90**, 015001 (2018).

[14] Y. Baum, T. Posske, I. C. Fulga, B. Trauzettel, and A. Stern, Phys. Rev. B **92**, 045128 (2015).

[15] Y. Baum, T. Posske, I. C. Fulga, B. Trauzettel, and A. Stern, Phys. Rev. Lett. **114**, 136801 (2015).

[16] A. A. Burkov, Phys. Rev. Lett. **120**, 016603 (2018).

[17] A. A. Burkov, Phys. Rev. B **97**, 165104 (2018).

[18] A. A. Burkov and L. Balents, Phys. Rev. Lett. **107**, 127205 (2011).

[19] A. A. Burkov, Phys. Rev. Lett. **113**, 187202 (2014).

[20] D. T. Son and B. Z. Spivak, Phys. Rev. B **88**, 104412 (2013).

[21] A. Altland and M. R. Zirnbauer, Phys. Rev. B **55**, 1142 (1997).

[22] C. Kallin, Rep. Prog. Phys. **75**, 042501 (2012).

[23] G. E. Volovik, *The Universe in a Helium Droplet* (Oxford University Press, Oxford, 2003).

[24] M. Cheng, R. M. Lutchyn, V. Galitski, and S. Das Sarma, Phys. Rev. Lett. **103**, 107001 (2009).

[25] N. Read and D. Green, Phys. Rev. B **61**, 10267 (2000).

[26] G. Sundaram and Q. Niu, Phys. Rev. B **59**, 14915 (1999).

[27] F. D. M. Haldane, Phys. Rev. Lett. **93**, 206602 (2004).

[28] P. Středa, J. Phys. C **15**, L717 (1982).

[29] D. J. Thouless, M. Kohmoto, M. P. Nightingale, and M. den Nijs, Phys. Rev. Lett. **49**, 405 (1982).

[30] R. B. Laughlin, Phys. Rev. B **23**, 5632 (1981).

[31] We imagine $p + ip$ superconductivity as being induced by proximity to a strong s-wave superconductor. We thus do not consider the self-consistency condition and dependence of the amplitude $|\Delta|$ on the flux Q.

[32] I. M. Lifshitz, Sov. Phys. JETP **11**, 1130 (1960).

[33] G. E. Volovik, Phys. Usp. **61**, 89 (2018).

[34] The Hall conductivity is still nearly quantized deep in the topological phase [19] with corrections being small in the parameter k_F/k_W (Fermi momentum over the distance between the nodes). However, at the transition $k_W \to 0$, the corrections are not small and σ_{xy} evolves continuously.

[35] N. Nagaosa, J. Sinova, S. Onoda, A. H. MacDonald, and N. P. Ong, Rev. Mod. Phys. **82**, 1539 (2010).

[36] N. Nagaosa, J. Phys. Soc. Jpn. **75**, 042001 (2006).

[37] N. A. Sinitsyn, A. H. MacDonald, T. Jungwirth, V. K. Dugaev, and J. Sinova, Phys. Rev. B **75**, 045315 (2007).

[38] S. Li, A. V. Andreev, and B. Z. Spivak, Phys. Rev. B **92**, 100506 (2015).

[39] I. Ado, I. Dmitriev, P. Ostrovsky, and M. Titov, Europhys. Lett. **111**, 37004 (2015).

[40] V. M. Yakovenko, Phys. Rev. Lett. **98**, 087003 (2007).

[41] E. J. König and A. Levchenko, Phys. Rev. Lett. **118**, 027001 (2017).

[42] X. Ying and A. Kamenev (to be published).

[43] D. Khmelnitskii, JETP Lett. **38**, 552 (1983).

[44] A. M. M. Pruisken, in *The Quantum Hall Effect*, edited by R. E. Prange and S. M. Girvin (Springer-Verlag, New York, 1987).

[45] H. P. Wei, D. C. Tsui, and A. M. M. Pruisken, Phys. Rev. B **33**, 1488 (1986).

[46] M. Bocquet, D. Serban, and M. Zirnbauer, Nucl. Phys. **B578**, 628 (2000).

[47] A. Altland, D. Bagrets, L. Fritz, A. Kamenev, and H. Schmiedt, Phys. Rev. Lett. **112**, 206602 (2014).

[48] Other examples include class C in 2D which works exactly the same as class D. At the same time, class A in 2D (anomalous Hall effect and Haldane model) does not show a symmetry-protected sharp transition due the lack of symmetry.

[49] C. W. Groth, M. Wimmer, A. R. Akhmerov, and X. Waintal, New J. Phys. **16**, 063065 (2014).